Published in final edited form as:

Zhang, S., Du, Q., Cheng, K., Antonietti, M., & Yang, F. (2020). Efficient phosphorus recycling and heavy metal removal from wastewater sludge by a novel hydrothermal humification-technique. Chemical Engineering Journal, 394: 124832. doi:10.1016/j.cej.2020.124832.

Efficient Phosphorus Recycling and Heavy Metal Removal from Wastewater Sludge by a Novel Hydrothermal Humification-Technique

Shuaishuai Zhang, Qing Du, Kui Cheng, Markus Antonietti, Fan Yang

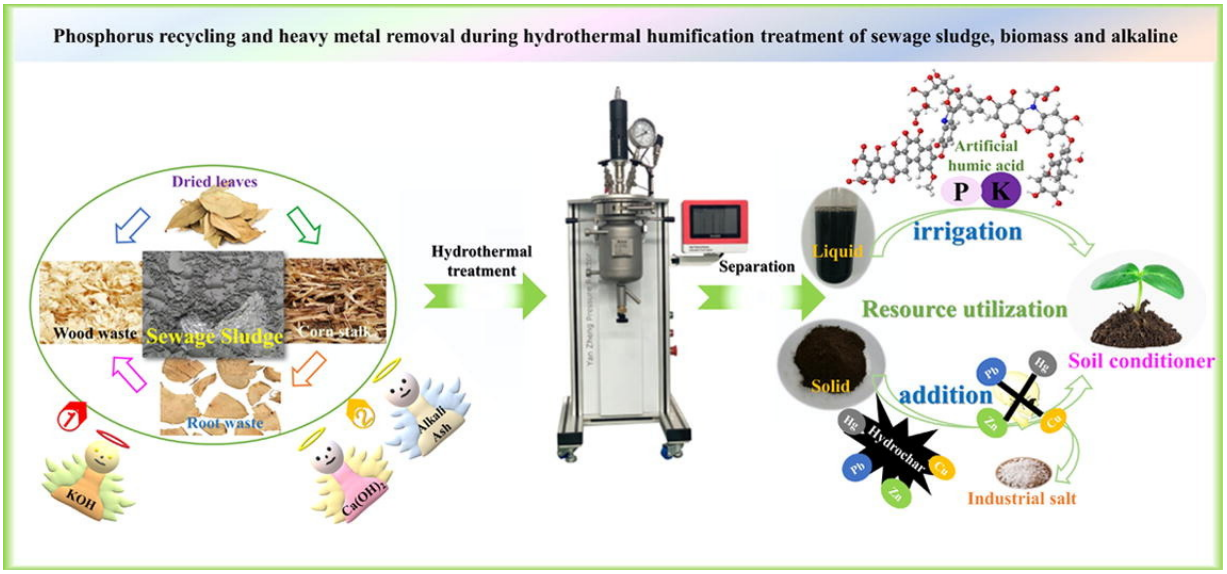

Efficient Phosphorus Recycling and Heavy Metal Removal from Wastewater Sludge by a Novel Hydrothermal Humification-Technique

Shuaishuai Zhang[a], Qing Du[a,b], Markus Antonietti[c,#], Fan Yang[a,b,*]

[a] *Joint laboratory of Northeast Agricultural University and Max Planck Institute of Colloids and Interfaces (NEAU-MPICI), Harbin 150030, China.*

[b] *School of Water Conservancy and Civil Engineering, Northeast Agricultural University, Harbin 150030, China.*

[c] *Max Planck Institute of Colloids and Interfaces Department of Colloid Chemistry 14476 Potsdam (Germany).*

[*] Corresponding author: yangfan_neau@163.com

[#] Corresponding author: Markus.Antonietti@mpikg.mpg.de

Abstract

This publication is presenting a simple and low-cost hydrothermal humification (HTH) treatment of sewage sludge (SS) together with alkali ash and biomass for simultaneous implementation of heavy metal removal, nutrient recovery (P) and ash refining. Analysis of the products indicate that dehydration and decarboxylation under hydrothermal conditions are the elemental reactions leading to sludge/biomass decomposition and artificial humic matter formation. Importantly, introduction of plant biomass into sludge-derived samples and adjustment of alkali ash mass effectively improved the recovery of the P element, realizing high contents of dissolved phosphorus (DP) (from 7045 to 10075 mg/L) at appropriate pH values (6.5-7.7). In addition, the drop of the Cr and Cd content below detection limit together with a sharp decrease of the elements Cu (0.07-0.46 mg/g), Zn (0.15-0.98 mg/g) and Pb (0.067-0.142 mg/g) after HTH treatment is observed from sludge-derived liquid products. Pot planting experiments are conducted to investigate the P-availability in both sludge-derived liquids and solids for promotion of plant growth. A higher proportion of shoot-to-root weight (62.1 % versus 46.2 %) and preserved moisture contents (84.7 % versus 83.7 %) when compared to the control groups demonstrate the effect of the presence of more nutrients after addition of sludge-derived liquid products.

Keywords: Sludges; Hydrothermal humification; Phosphorus recycling; Heavy metal removal; Fertilizer.

1. Introduction

The amount of collected and as such available sewage sludge is increasing due to rapid introduction of wastewater treatment plants in developing countries. Worth noting, the large

absolute amount of phosphorus (P) in sewage sludge has already attracted much attention as an important secondary resource of phosphorus recovery. The world's resources of plant-available phosphates are limited, but the demand for phosphate fertilizer in agricultural production is increasing, so that phosphate will turn into a restricted resource rather soon[1]. Hence, in order to guarantee increased crop yields and food supply for the world's population, research on other secondary sources of phosphorus is necessary[2]. On the other hand, side products of the food chain of wastewater sludges contain large absolute quantities of P, and it is a duty to develop technologies for recovering phosphorus from such waste streams to close the phosphorus loop and treat this element in a sustainable fashion[3].

In the present context, the large amounts of macronutrients (N, P, K, Na, Ca, Mg, etc.) in sludge beneficial for plant growth are important, and it is the reason why agricultural use is traditional. Modern sludge however contains leftovers of drugs, hormones, prions, pathogenic microorganisms, parasite eggs, and partly too high concentration of heavy metals (Cu, Pb, Hg, Zn, Cd, Cr, etc.), which are then given directly back to the food chain, thus prohibiting nowadays the direct use of sludge in agriculture[4]. Control of heavy metals in original sludge always remain challenging, and their presence provides a potential environmental risk [5]. Hence, in order to obtain a stable, low-pollution, and beneficial amendment for soil and to close the phosphate loop, sewage sludge needs to be properly treated prior to application.

With this target, over the past few years techniques have been introduced in an attempt to heavy metal removal and P recovery from sewage sludge, sludge ash or digester supernatant, including thermal treatments[6, 7], bioleaching methods[8, 9], chemical extraction[10, 11] and electrodialytic methods[12, 13]. These projects are economically not feasible due to their complex processes for phosphorus recovery. Among all these techniques, hydrothermal treatment can be considered to be one of the most simple and rapid methods: the applied autogenous pressure environment and medium high temperature (180-220 °C) are ideal for pathogens inactivation, prion decomposition, and effective decomposition of proteins and most drugs into inactive follow-up products[14]. Moreover, the hydrothermal processing can significantly improve the occurrence of dehydration, decarboxylation and condensation of wet sludge [15] and thereby the ability to dewater it more easily. In this regard, Xu et al. [16] focused on the migration and transformation mechanisms of phosphorus during the hydrothermal treatment of sludge. A study by Wang et al.[17] described that the hydrothermal treatment can achieve deep dewatering of the sludge, and the produced hydrochar can be used as a soil conditioner.

A newly developed hydrothermal humification (HTH) progress[18] can be considered as a green, economical route for production of humic substances. In the present work, we apply HTH to sludge, with the purpose of sterilizing, digesting and dewatering it, as well as to improve

phosphor solubilization. In order to reduce the cost of conventional alkaline activators (e.g. KOH and NaOH), alkaline plant ashes or coal combustion ashes can be alternatively employed. We will employ both OH-sources to compare and to realize an "all-waste-strategy" for sludge valorization, with the added benefit that plant ashes of course contain additional micronutrients which are then also recovered. This HTH strategy can therefore be seen as a first step to provide an integrated optimized disposal route, realizing an efficient utilization of sludge resources, nutrient recovery and heavy metal separation, but also producing an effective fertilizing vector for the promotion of plant growth.

2. Materials and methods

2.1. Materials and Reagents

Sewage sludge (SS) used in the experiment was collected from a wastewater treatment plant located in Wuhan, China and oven-dried at 105 °C until constant weight. Alkaline combustion ash (AA) was collected from a factory located in Shenzhen, China, with the metals Na, Al, Ca and Fe as the main metal contaminants. Basic composition and physicochemical of SS and AA properties are listed in Table 1. The soil used for the pot experiment was a topsoil (0-15 cm) collected from Harbin, China. Cellulose, potassium hydroxide (KOH), calcium hydroxide ($Ca(OH)_2$), hydrochloric acid (HCl), hydrofluoric acid (HF) and perchloric acid ($HClO_4$) were provided by Tianjin Chemical Reagent Co., Ltd, China. All reagents and chemicals were used as received without further purification. Deionized water (DI, 18.2 MΩ cm) was used for all experimental solutions.

Table 1. Initial characteristics of sewage sludge (SS) and alkaline ash (AA).

Feedstock	Parameter	Value
Sewage sludge (SS)	pH	7.4
	Moisture content (%)	86.0
	Organic matter content of solid (%)	55.7
	Total *phosphorus in the* dried *s*ewage sludge (mg/g)	75.0
	Total potassium in the dried sewage sludge (mg/g)	18.2
Alkaline Ash (AA)	Total *phosphorus in the* ash (mg/g)	79.3
	Total potassium in the ash (mg/g)	14.3

2.2 Procedures

Controlled amounts of SS (without further drying), biomass (B) ((cellulose (C), root waste (R), wood waste (W), corn stalk (CS), and dried leaves (L)), and different masses of KOH (to ensure that the molar ratio between integrated sugar content and KOH in the final recipe is close to 1) were dispersed in deionized water and transferred to a 50 mL Teflon-lined autoclave, then heated to 200 °C for 24 h. After slow cooling to room temperature, the final dispersions were separated from the liquid phase by ordinary centrifugation at 8000 rpm for 5 min. Samples were denoted as SS+B+KOH (B=C, R, W, CS and L). In another set of experiments, KOH was replaced by alkaline ash (with $Ca(OH)_2$ addition for caustification) to carry out the "all-waste" experiments, and the samples were denoted as SS+B+AA (B=C, R, W, CS and L). The liquid phase was diluted into the detection range of ICP-AES testing for P, K, Cu, Zn, Pb and Hg content. Samples of the sediment (centrifuged and dried) were analyzed for P, K, Al, Na, Ca, Cr, Fe, Cu, Zn, Cd, Hg and Pb content, with following acidic leaching for separation of hydrochar and heavy metal ions. Further, recovery of heavy metals via reduction reaction was explored in addition. Other detailed experiment procedures can be found in the Supporting Information.

3. Results and discussion

Fig. S1 gives pictures of the original sludge, alkaline ash, liquid and solid products after HTH treatment. As seen, SS appears darkish grey, liquids and solids as products of sludge after HTH treatment exhibit the typical, charming black colour of humic acid-based products. SEM examinations were used to get a visual sense for the changes in the microstructure throughout sludge digestion with and without the HTH process in presence and absence of added biomass and alkali source (KOH). The data are presented in Fig. 1, Fig. S2 and Fig. S3. The dried sludge particles with rough surfaces and narrow channels are in a range of 50-100 μm, and of very

heterogeneous nature (Fig. S2a-b). Pure sludge after HTH (Fig. S3a-b) turned out not to be able to form humic acids in significant parts (Fig. S3c-d), as obviously the saccharide content is too low. Instead, a gluey, smelly, alkaline hydrolysate is obtained, which is not along the strategies of this paper or even useful. The SEM pictures depict only a minority component of solid minerals, which are contained in the sludge and refund at the end.

This is the reason why we added >50 wt% of another carbohydrate-based biomass waste to form hydrothermally the humic acids in the presence of the hydrolyzing sludge, and the resulting products have weak smell, nice texture, and are easy to handle. The structural change of the products reflects the decomposition of carbohydrate matter during hydrothermal treatment. Using cellulose as the secondary compound (which completely hydrolyzes into glucose), the as-formed weak fulvic acids cannot effectively bind fatty acids (one of the main organic ingredients of sludge), leaving a pungent smell (Fig. 1a-b). The best rebinding of organic fragments into A-HA occurs when a lignin containing secondary biomass is added to the sludge, e.g. wood powders, dried leaves or root leftovers (Fig.1c-h). At these starting compositions, the hydrothermal treatment can improve sludge and organic matter decomposition, which is very important for P migration and transformation, and two rather clean products, a black humic solid phase and a black liquid phase, are obtained. In this way, very positive properties can be realized, as described later.

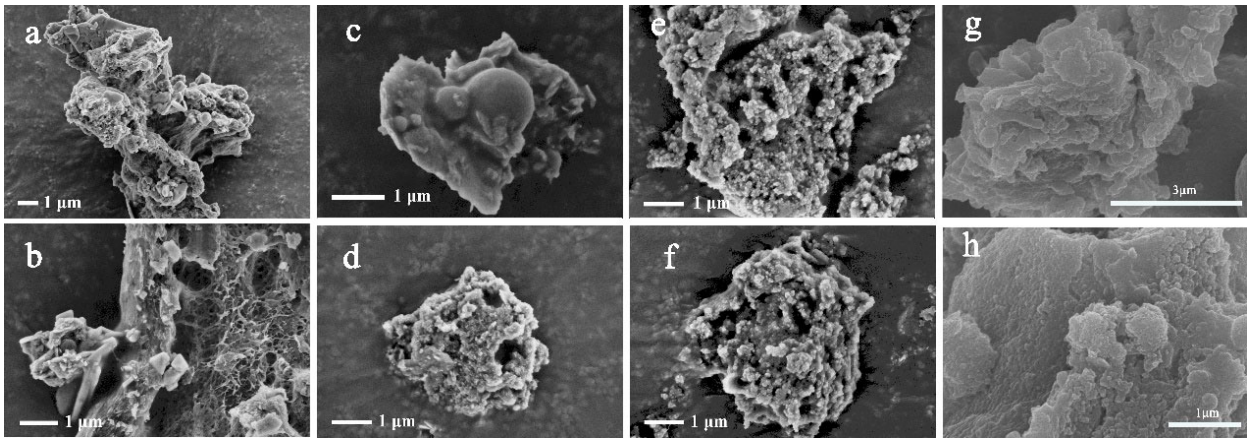

Fig. 1. SEM images of SS+C+KOH (a, b), SS+W+KOH (c, d) SS+R+KOH (e, f) and SS+CS+KOH (g, h) after HTH process.

The high P content (7.5 wt%) contained in dried sewage sludge is distributed between inorganic mineral particles and the abundant organic matter which acts as an adhesive between the minerals to form compact, sticky structures. After alkaline-HTH treatment, approximately 60 % of the primary weight are in the solid leftover, mainly minerals conjugated with the A-HA, which experienced a profound alteration of the morphology with visible etching marks on their surfaces (Fig. 1c-h), resulting from the interaction with humic substances. Similar morphological changes were already found in a different context and could be clearly deduced to the mineral-humin interactions [19]. Interestingly, also rather porous “card-house” like structures are found in the in sludge-derived solids metals, which we attribute to recrystallized clay sheets, interlinked by metal-

precipitated humic matter (Fig. S4). Such tectonic pores are good for water uptake and air permeation of the soil, promote space for microbial growth [20], and have great importance for land application of sludge products.

Application of alkali ash (a typical solid waste from biomass firing) to replace KOH (an industrial chemicals) provides a new "win-win" strategy, as it not only decreases the cost of sludge treatment, but also realizes alkali ash refining. In order to enhance the alkalinity of ash for more effective transformation, $Ca(OH)_2$ is chosen as an auxiliary to participate in HTH process. Ca^{2+} can bind the many multivalent anions such as CO_3^{2-} and SO_4^{2-} in ash and increases the activity of OH- ("caustification"). The structural texture of the alkaline ash (Fig. S2c-d), mostly consists of spherical particles with different sizes from the nanoscale to the microscale, as typical for flame processes and contains a broad diversity of constituent species (mainly metal bicarbonates, carbonate, oxides and hydroxides). After addition of humin-forming, secondary biomass, stronger disintegration of sludge precursors is observed in SEM images (Fig. S5c-h). The extent of change depends on the type of biomass precursors, and obvious reconstitution can be observed also for wood and root powders. In all four samples, it is observed that some patch-like materials adhere to the etched surfaces of minerals, implying the adhesive interactions between A-HA and minerals.

The element (C, H, O, N, S) composition analysis of the solid phase and yield of humic substances in the liquid residues of hydrothermally treated sludge samples in absence and presence of different secondary biomasses are summarized in Table S1, along with pH value of solution. The solid product removed from the treated SS is characterized by an (expectedly) low carbon content with a content of C, H and O of 0.97 %, 1.56 % and 60.69 % (the leftover minerals of the oxygen in ash content as determined by TGA analysis, including 7.63 % of oxygen carried by organic matter), respectively, i.e. the organic content of sludge is mostly in the water phase. Ash clearly is mostly mineralic (83.23 %), as it is the product of a combustion process removing organic material, the remainder presumably being adsorbed or chemically bound water and CO_2. It is obvious that the contents of C, H, O, N and S in the sludge-derived samples is significantly increased after biomass conjugation, i.e. also the precipitated material contains larger amounts of bound carbon. The molar ratios (H/C, O/C and C/N) as calculated are generally used to determine the carbonization-degree[4], but are to be taken in complex mixtures with a grain of salt. Both ratios (H/C and O/C) of the obtained solid materials significantly decrease after the introduction of base and biomass, reflecting stronger carbonization and higher condensation. The tendency of the molar ratios of C/N in the solid materials was similar to the molar ratios of H/C and O/C, moreover, the increase of N content in SS+AA, SS+B+KOH and SS+B+AA may be ascribed to the products from protein decomposition of exogenous biomass[21]. Fig. 2a represented the H/C and O/C atomic ratio in a scatter diagram of sludge-derived samples, and different treatments with

the three added secondary biomass precursors are shown for comparisons.

According to the Van-Krevelen diagram, dehydration and decarboxylation are the basic reactions resulted in the decomposition of sludge during HTH reaction[22]. As seen, SS+B+KOH and SS+B+AA samples were mainly located at the O/C of 0-0.6 and the H/C of 0.7-2.2. The contents of remaining H and O were only 1.09 wt%, and 0.09 wt% in AA, respectively (data measured by EA).

Obviously, many parameters of sludge/biomass-derived samples are very similar, favorably supporting the concept that the combination of AA and $Ca(OH)_2$ can have a same effect as a harsh base. Yields of humic acids extracted from liquids (0.015 % to 0.020 %) can be obtained, which are much lower than those in the absence of sludge (i.e. 1.2 % for wood as an example), suggesting that the humic substances take up heavy metals and multivalent cations, adsorb the sludge hydrolysates, and precipitate practically completely towards the formed solids. Humic acid can indeed effectively chelate heavy metal ions. Usharani and Namasivayam[23] studied that the effect of humic acid on the removal of heavy metals in sewage sludge, and already their results showed that humic acid can be effectively used to bind the heavy metal in sewage sludge, which is helpful for soil amendment.

Comparative XRD patterns can help to identify the crystalline phases of a series of solid products and are presented in Fig. 2b. In brief, the peaks of minerals in all samples were labelled with number symbols. XRD analysis indicated that the major elements in the crystalline part of the original sludge are Si, Ca, Al, Fe and P, and the strong peak around 26.7° in all samples is attributed to quartz (SiO_2), originating from the sandy nature of aquatic sludges (highlighted in the figure)[24]. Typically, insoluble $CaPO_3(OH)\cdot 2H_2O$ is the main crystal phase appearing in dried sludge, which is obviously decreased in the series of hydrothermally treated products, while several new peaks show up in the scattering curves, being assigned to the presence of as-generated $CaFe_5O_3$, $Ca_{1.5}HP_2O_7$, $Ca_4Fe_9O_{17}$ and $AlPO_4$. This indicates the profound transformation of phosphorus into new species also in the minor solid phase during the hydrothermal treatment process.

Interestingly, as that HTH treatment not only mimics natural geochemical processes, but also provides a smart fertilization route, namely, formation of all three-classes of P resources for plant growth[25]: (1) soluble molecular and amorphous phosphate for immediate fertilization; (2) hydrated Calcium phosphates and metaphosphates for intermittent, retarded effects; and (3) Al-P bonding as a slow release P sources. In a similar work, Xu et al[16] investigated the effects of temperature, time, pH, and CaO on phosphorus migration and transformation during hydrothermal treatment, and the results found that in the solid products non-apatite-inorganic phosphorus gradually transformed into apatite with the increase of hydrothermal temperature. By adding CaO,

the complete transformation from non-apatite-inorganic phosphorus to apatite was observed. Furthermore, no peaks attributed to heavy metals were detected by the XRD analysis due to their relatively low concentration.

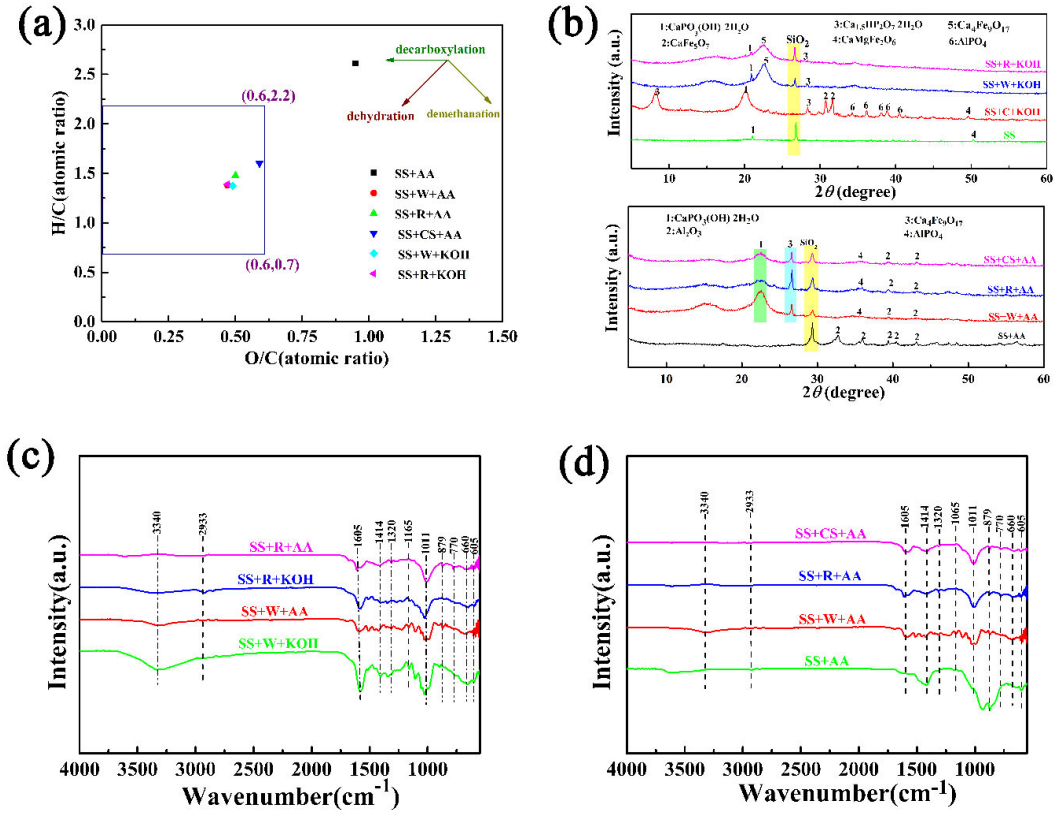

Fig. 2. (a) Van Krevelen diagram, (b) XRD patterns and (c, d) FTIR spectra of a series of sludge-derived samples.

FTIR spectra were used to identify the chemical functional groups of as-prepared solid residues after the HTH process, as depicted in Fig. 2c-d; a summary of characteristic peaks is listed in Table S2. Profiles of SS+B+KOH and SS+B+AA samples (Fig. 2c-d) looks very similar, thus, it could be verified again that AA is able to replace KOH. Absorption in the region of 3340 cm^{-1} can be assigned to the presence of water, alcohols, phenols and acids, are mostly generated by the decomposition of biomass and SS[26]. The peaks at 2933 cm^{-1} correspond to C-H stretching vibration (-CH_3, -CH_2), showing the presence of aliphatic fatty acids from sludge in the samples[27]. The peaks at approximately 1605 cm^{-1} correspond to C=C stretching vibration (aromatic rings), C=O stretching vibration (ketone, aldehyde, carboxyl, ester) and -CONH- stretching vibration (amide bonds) and are indicating the presence of organic entities that come from proteins in the SS and added biomass[28]. The peaks at 1414 and 1320 cm^{-1} were attributed to the C=C stretching vibration and C-H stretching vibration (-CH_3, -CH_2), respectively. The peak at 1165 cm^{-1} results from the C-O stretching vibration of alcohol, ether, ester and carboxyl. In addition, the absorption band at low wavenumber (i.e. 1011 cm^{-1}) may be assigned to Si-O-Si asymmetric stretching in silicates. Characteristic bands around 605 cm^{-1} were due to the O-P-O

bending vibrations, and the band at around 660 cm^{-1} is related to inorganic functional groups[29]. All these bands are typical for all samples and are also fully consistent with the results that have been reported by other researchers[30].

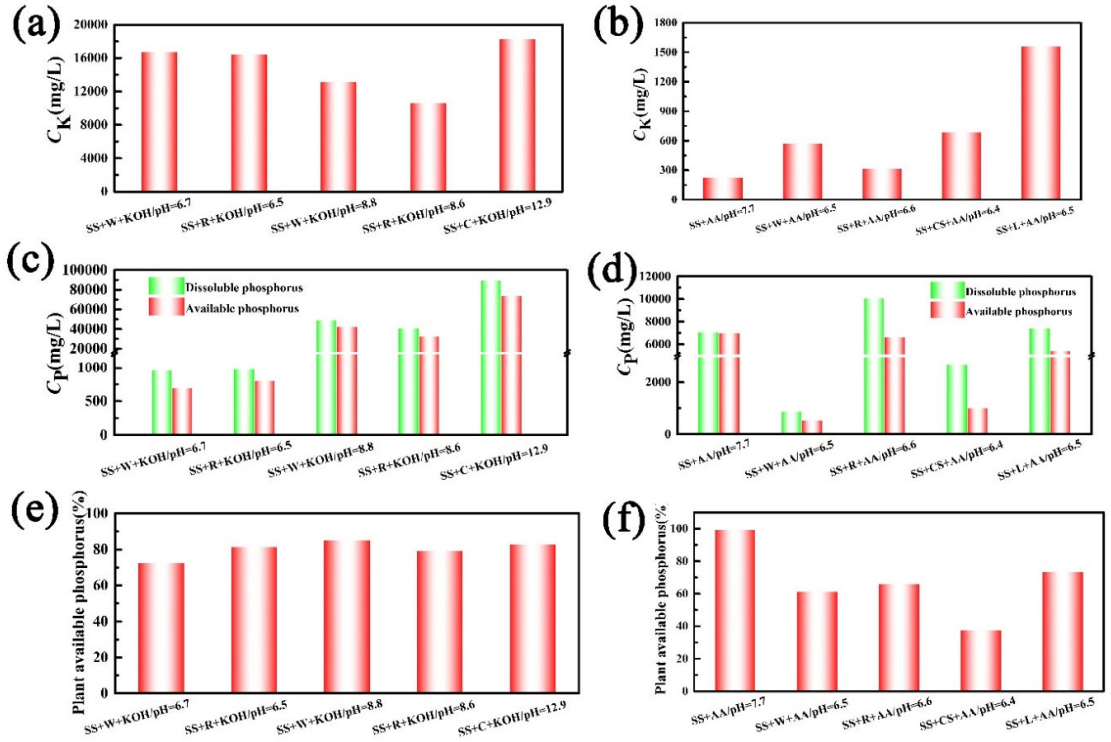

Fig. 3. Variations of (a, b) K, (c, d) P element and (e, f) ratios of AP to DP in the supernatant of a series of sludge-derived samples.

Focusing now on the liquid phase, the amounts of K in SS+AA, SS+B+KOH and SS+B+AA samples are shown Fig. 3a-b. Notably, a slight increase of pH value, even for KOH, may decrease concentrations of K^+ ions in solution, as more base facilitates the formation of more carboxylate groups also at the solids, that way enhancing the enrichment of K ions on the surface of the humic acids through counterion effects.

Fig. 3b displays successful examples of sludge recycling and ash refining via HTH treatment, leading to sharp decline of K ions in the liquids. During the hydrothermal treatment of sludge, some K also will be released into the liquid as the cell ruptures. Adding the secondary biomass precursors (wood, root, corn straw and leaves) for humic acid formation, various effects on K leaching are observed, and leaves perform the best yield based on high production of humic acids with largest molecular weight (81300 g/mol) and strongest total acidity (10.0 mmol/L), due to the humic acid produced by the leaves contains many acidic functional groups (mainly carboxyl and hydroxyl groups) which can effectively interact with K^+, as presented in our previous work [31].

Comparing the different pH values of solutions after hydrothermal reactions, the pH value in the solution after the reaction of SS+C+KOH is too high. Pointing to conversion problems, i.e. the cellulose does not completely react with KOH under the given conditions. We assume that KOH

and SS indeed reacts faster, equivalent to the previously described alkali activation of SS, and the resulting intermediary fatty acid salts are simply not basic enough to promote cellulose digestion. On the contrary, the pH value in solution of SS+B+KOH after the reaction is closer to neutral, and the possible reasons for SS/KOH/biomass is now that biomass reacts as fast as the SS, and significant parts of the alkaline are now indeed invested in carbohydrate splitting towards carboxylates, that lowering the pH value to about neutral.

Fig. 3c provides information that the P uptake in the aqueous phase is directly related to increasing solution alkalinity, only a slight increase in pH value (6.7-8.8) brought a more than forty times high phosphorus content (from 962 mg/L to 49595 mg/L as taken SS+W+KOH as an example). In general, Fe, Al and Ca oxides are the major cations buffering the phosphate solubility in soils, Fe and Al-containing minerals have the dominant role under acidic conditions, while Ca minerals rule in alkaline soils. Satisfactorily, alkali ash, as the source of basicity and P (79.3 mg/g), enables high contents of dissolved phosphorus (DP) (7045 to 10075 mg/L) and appropriate pH value (6.5-7.7) (Fig. 3d), all at the same time, that is the degradation rates of SS and biomass are nicely balanced, and the final product can be directly used without pH adjustment. A simultaneous larger amount of $AlPO_4$ formed in SS+B+AA samples (Fig. 2b) coming from the aluminium species in the combustion ashes enable the preparation of graded P fertilizer for long-term supply to soil. Interestingly, the dissolution of $AlPO_4$ is known to depend on microorganisms in the soil. Illmer et al[32] showed that four microorganisms (aspergillus niger, penicillium simplicissimum, pseudomonas sp. (PI18/89) and penicillium aurantiogriseum) do promote solubilization of the otherwise hardly-soluble $AlPO_4$. Moreover, P availability in soils is reported to be at maximum at the pH value of 6.5[33].Therefore, the pH of the obtained reaction solution is effective for the absorption of phosphorus by plants in the soil. Significant differences in the ratios of AP to DP are observed when comparing the SS+B+KOH and SS+B+AA series, being influenced by as-formed P species (Fig. 3e and 3f).

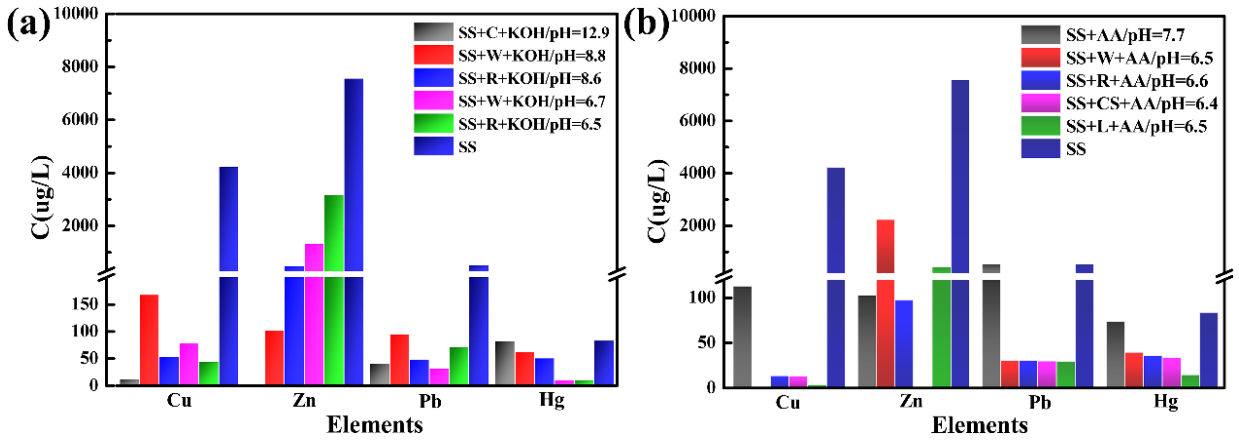

Fig. 4. Variations of heavy metal concentrations in the supernatant of a series of sludge-derived samples.

By purpose, we use HTH instead of hydrothermal digestion or hydrothermal carbonization, as the in-situ formed loose humic chains are favorable adsorbents for heavy metals from liquids. If appropriately formulated, metal complexation of the units will lead to destabilization and precipitation during HTH treatment, thus enabling simple separation for subsequent recovery of heavy metals from the fertilizing phase. A possible combustion of the solid, metal containing, black carbonaceous matter then gives energy and produces ashes as “industrial salts”, either for compact deposition or for recycling. The condensation towards humic acids will also bind all nucleophilic volatiles by co-condensation, and only a few inert, less active smells stay unaffected. Heavy metal content is another important factor to be considered in sludge valorization, and it is necessary to minimize the amounts of heavy metals in hydrothermal liquids to enable their direct use as a liquid fertilizer. To determine the influence of the hydrolysis, humification, and crystallization process, the whereabouts of the element, Cu, Zn, Cd, Hg and Pb were analyzed. The initial contents in the original dried sludge were determined to be 0.91, 1.69, 0.004, 0.08 and 0.136 mg/g, respectively (Table 2). Obviously, Cu, Zn and Pb are the predominant heavy metals. Table. S2 lists the concentrations of selected elements in the technical combustion ash, and here, Cr, Cu, Zn and Pb are dominant species with relatively lower contents of Cd and Hg.

In China, according to Chinese National Environmental Standard quality (National Standard GB 4284-2018, China) for usable sludge in agriculture (cultivated land, gardens and pastures), heavy metal concentrations should be controlled to be under the critical content of 0.5, 0.5, 1.2, 0.003, 0.003 and 0.3 mg/g for Cr, Cu, Zn, Cd, Hg and Pb, respectively. Apparently, the original sludge used in this paper cannot meet the standards, however, the almost undetectable existence of Cr and Cd elements together with a sharp decrease of Cu (0.07-0.46 mg/g), Zn (0.15-0.98 mg/g) and Pb (0.067-0.142 mg/g) elements after HTH treatment result in aqueous products with a much lower concentration than stipulated by the national standard. This is due to absorption into the condensed humic acid structure, electrostatic interaction with phenols and carboxylates on hydrochar and humic substances[34] and precipitation or complexation by OH- and other mineral

formers, all turning the metals practically exclusively into the solid phase. As an exception, Hg behaves rather unsystematic, which we attribute to the (here non-discussed) redox properties of humic matter. Oxidized mercury is soluble in water and easily adsorbed on solid surfaces, making the as-prepared hydrochar a superior choice for its capture, whereas Hg(0) is neither soluble in water nor easily adsorbed at surfaces, which can be the main reason of difficulties of its removal. If sludges are rich in heavy metals, it is obvious that the (in any case then minor) solid phase cannot be used for farming purposes. As it is less water-containing, compact and enriched in heavy metals, it might be even used for further recovery of industrial salts via combustion od the organic components.

Fig. 4 summarizes the variations of heavy metal concentrations in the supernatant of original sludge in our series of sludge-derived samples. All four heavy metal species are massively reduced after HTH treatment, and to a certain extent, almost complete removal of heavy metals has been achieved. Generally, removal efficiencies for heavy metals (except Hg) increased with higher concentrations of KOH (Fig. 4a). Fig. 4b shows the biomass type-dependent elimination of heavy meals replacing KOH with alkali ash. Despite the counterintuitive fact that we even added some heavy metals with the ash, superior performance of heavy metal removal is obtained. We found nearly complete elimination for Zn, Cu and Pb and 83 % of Hg removal with an at the same time pH neutral environment at the end. In direct comparison, the alkali ash as a recycling substitute of the strong chemical base has to be seen very positive, as it not only realizes resource utilization, but also shows better metal removal performance (98.8 % versus 99.6 % for Cu, 58.5 % versus 98.7 % for Zn, 86.7 % versus 94.4 % for Pb and 88.4 % versus 57.4 % for Hg on SS+R+KOH versus SS+R+AA sample). This can be to our opinion attributed to the recrystallization of the ash-contained inorganic elements (Al, Si, Ca and Fe) with heavy metals towards stable compounds with low solubililty[35]. Again, Hg removal efficiency is not perfect, i.e. it stays a special case even in the presence of ash.

The above results are in excellent agreement with those obtained from the group of Liang [36] (without ash addition), and they found that heavy metals in the sludge after hydrothermal treatment mainly remained in the solid phase. As seen, advanced hydrothermal treatment has a tendency to concentrate heavy metals to be bound into solid reaction products.

Table 2. Concentrations of elements in the solid residues of SS and its derivatives after HTH treatment.

	SS	SS+AA	SS+W+AA	SS+R+AA	SS+CS+AA	SS+W+KOH	SS+R+KOH
pH	7.4	7.7	6.5	6.6	6.4	6.7	6.5
P(mg/g)	75.0	29.73	35.11	35.03	35.08	38.58	31.42
K(mg/g)	18.32	5.273	5.925	6.155	5.201	14.45	15.90
Al(mg/g)	18.58	12.77	2.549	9.35	12.70	2.947	1.641
Na(mg/g)	10.8	19.86	1.719	17.31	16.33	18.93	20.23
Ca(mg/g)	20.01	49.84	18.64	22.81	25.51	1.060	1.651
Cr(mg/g)	0.15	0.087	-	-	-	-	-
Fe(mg/g)	16.04	19.57	2.81	11.64	10.40	2.61	1.38
Cu(mg/g)	0.91	0.46	-	0.07	-	0.14	-
Zn(mg/g)	1.69	0.98	0.15	0.86	0.24	0.29	0.19
Cd(mg/g)	0.004	-	-	-	-	-	-
Hg(mg/g)	0.08	-	-	0.07	0.13	-	-
Pb(mg/g)	0.136	0.142	-	0.067	0.101	-	-

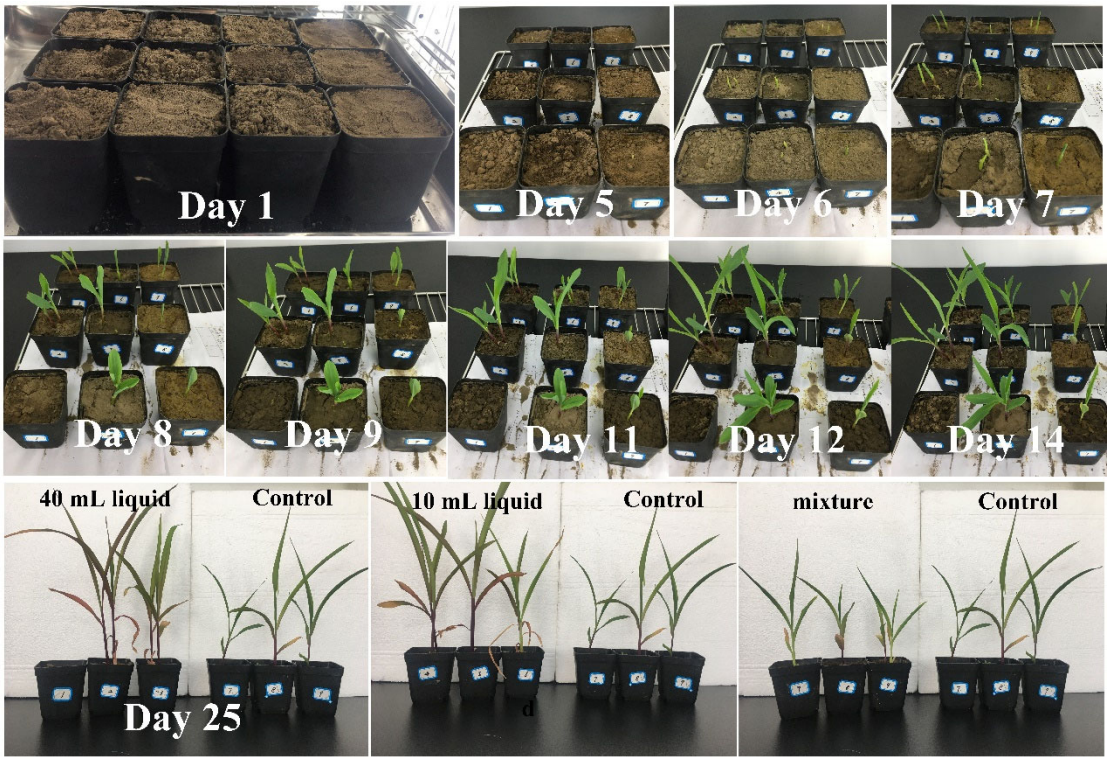

Fig. 5. Photos of seeding growth process of corn seeds at 25 days in black soils.

Finally, Fig. 5 depicts preliminary data on the seedling growth of corn in black soils (Harbin, China) after introduction of the different sludge-derived leaching liquids and mixtures of liquid

products and solid residues. Based on the above results, a series of SS+B+AA samples was chosen as the additive, due to high availability of nutrient elements and suitable pH value (close to soil pH). Clearly, growth promotion effects by sludge-derived liquids became evident already after 5 days of incubation, showing that plants have broken above the soil with some tiny sprouts. In the following cultivation process, we can watch the daily growth of the sprouts and see noticeable effects on plant growth by adding only 10 mL and 40 mL "sludge soup" while comparing with those of control groups. Notably, the addition of mixtures of liquids and solids is not providing positive effect on plant growth, but partly even retard their development. This may be due to overnutrition of solid residues (biochar) and liquids (primarily phosphorus, potassium and HA added to soil, which has to be confirmed by dolution experiments.

Comparative visible images reveal that both aboveground and belowground plant biomass was significantly higher in the groups treated by sludge-derived liquids compared to control groups (Fig. 6a) during the 25-day growth period, on the contrary, treatment with mixtures of solid and liquid sludge products (20 %) exhibits an obvious negative effect. Implementation of as-fabricated liquids obtained from HTH treatments increased soil available P on 1.43 times compared to the control groups (Fig. 6b), and AP contents in soils decreased with the extension of cultivation time, giving a good relationship with plant growth[37]. Moreover, introduction of mixed products only slightly increases the AP content (1.1 times than that of control groups). In addition, soil pH did not change across the treatments, presenting a mean neutral value.

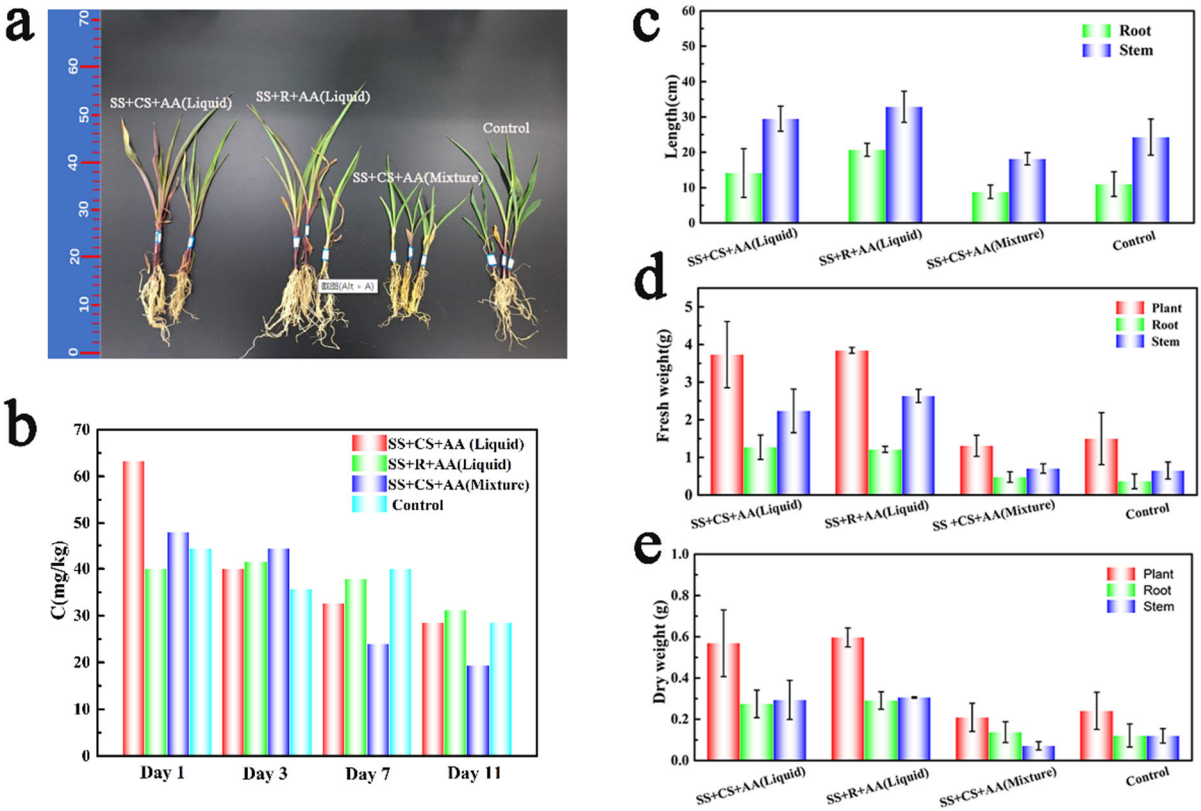

Fig. 6. Variations of (a) seedling growth (corn), (b) soil available P, (c) length, (d) fresh weight and (e) dry weight of root, stem and plant after 25 days of growth in black soils.

Fig. 6c shows that the length growth of corn root and stem was accelerated by exposure to sludge-derived liquid products. Among four samples, the groups treated with SS+R+AA liquid (only 10 mL) exhibit the best growth trend, because of high dissolved (10.08 g/L) and available P (6.65 g/L in AP) contents, which are 3.75 and 6.65 times higher than those of SS+CS+AA sample (40 mL). Lengths of root and stem were both greatly improved (on average 1.9- and 1.4-fold, respectively) when compared to the default experiments. Highest proportion of shoot-to-root (47.9 %, 62.1 %, 49.0 % and 46.2 % in the case of SS+CS+AA, SS+R+AA liquids, SS+CS+AA mixture and control groups) can be found in SS+R+AA treatment, showing increases in relative biomass allocation to aboveground. The group treated by mixtures is higher than that of control group, which may be because that A-HA addition reduces phytotoxicity and enhances root growth by adsorbing plant growth inhibitors on its surface, which can also alter the shoot-to-root ratio of plants [38]. For control groups (a relative nutrient-poor topsoil with 600 mg/kg total P), rhizosphere microbial activity is reduced in the case of plants grown under lower nutrient availability conditions, and plants typically invest more in the root biomass relative to the total plant biomass and have lower shoot-to-root ratios [39, 40].

Significant increases in fresh and dry weight (Fig. 6d and e) of both plant shoot and root biomass after application of sludge-derived liquids follows the improved plant nutrition due to the

co-location of various resources in the black liquids (K, P, humic substances as main ingredients). Obviously, the planting group treated by SS+R+AA liquid exhibits the best performance on these two key indicators, moreover, fresh and dry weights in all treatment groups are higher than that of control groups with average moisture contents of 83.7 % (mixture), 84.7 % (SS+CS+AA liquid), 83.3 % (SS+R+AA liquid) and 83.7 % (control), revealing that the as-prepared growth vector can promote water uptake by plants, as shown in Fig. S6. Interestingly, the mixture treatment group has stronger facilitation effect for water adsorption than that of control group, meanwhile, moisture content showed the highest value of 89.6 % on stem among all groups, implying that this treatment accumulated more nutrients and water uptake in the early growth stage (25 days) of corn seedlings. It is assumed that this indicates obvious promoting advantages in long-term cultivation periods, which however is subject of future studies. We nevertheless can conclude that the sludge-derived products after HTH treatment containing abundant nutrients and eco-friendly hydrochar could indeed represent a versatile soil fertilizer in agricultural production, while closing the phosphor cycle and the ash nutrition cycle at the same time.

Supporting Information

Methods: SI-1a. P-availability examination; SI-1b. Acid digestion; SI-2. Analytical methods.

Figures and Tables: Fig. S1. Visual images of original sludge (a), alkali ash (b), as-prepared liquid (c) and solid products (d) derived from sludge; Fig. S2. SEM images of original sludge (a-b) and alkali ash (c-d); Fig. S3.SEM images of SS (a, b) and SS+KOH (c, d); Fig. S4. SEM image of porous structure in sludge-derived solids (SS+R+KOH) after HTH process; Fig. S5. SEM images of the remaining minerals from SS+AA(a-b), SS+W+AA(c-d), SS+R+AA(e-f) and SS+CS+AA(g-h); Fig. S6. Comparative results of moisture contents in parts of corn seedings with and without treatment of sludge-derived products; Table. S1. Comparative elemental composition of dried SS, SS+AA, SS+B+KOH, SS+B+AA samples; Table. S2. Functional groups for solid residue based on FTIR spectra; Table. S3. Total concentrations of selected metals elements in alkaline ash.

AUTHOR INFORMATION

Corresponding Author

Fan Yang: telephone No: +86 451 55191528; fax No: +86 451 55191528; email: yangfan_neau@163.com.

Markus Antonietti: email: Markus.Antonietti@mpikg.mpg.de.

Conflicts of interest

There are no conflicts to declare.

Acknowledgements

The authors appreciate the financial support from the Natural Science Foundation of Heilongjiang Province of China (QC2018019), the financial support from University Nursing Program for Young Scholars with Creative Talents in Heilongjiang Province (UNPYSCT-2017018), National Natural Science Fund for Young Scholars (31600413).

References

[1] M. Atienza–Martínez, G. Gea, J. Arauzo, S.R.A. Kersten, A.M.J. Kootstra, Phosphorus recovery from sewage sludge char ash, Biomass Bioenergy 65 (2014) 42-50. https://doi.org/ 10.1016/j.biombioe.2014.03.058.

[2] C. Blocher, C. Niewersch, T. Melin, Phosphorus recovery from sewage sludge with a hybrid process of low pressure wet oxidation and nanofiltration, Water Res 46 (2012) 2009-2019. https://doi.org/ 10.1016/j.watres.2012.01.022.

[3] H. Herzel, O. Kruger, L. Hermann, C. Adam, Sewage sludge ash--A promising secondary phosphorus source for fertilizer production, Sci Total Environ 542 (2016) 1136-1143. https://doi.org/ 10.1016/j.scitotenv.2015.08.059.

[4] X. Wang, Q. Chi, X. Liu, Y. Wang, Influence of pyrolysis temperature on characteristics and environmental risk of heavy metals in pyrolyzed biochar made from hydrothermally treated sewage sludge, Chemosphere 216 (2019) 698-706. https://doi.org/10.1016/j.chemosphere.2018.10.189.

[5] S. Van Wesenbeeck, W. Prins, F. Ronsse, M.J. Antal, Sewage Sludge Carbonization for Biochar Applications. Fate of Heavy Metals, Energy Fuels 28 (2014) 5318-5326. https://doi.org/10.1021/ef500875c.

[6] Z.A. Saleh Bairq, R. Li, Y. Li, H. Gao, T. Sema, W. Teng, S. Kumar, Z. Liang, New advancement perspectives of chloride additives on enhanced heavy metals removal and phosphorus fixation during thermal processing of sewage sludge, J. Cleaner Prod. 188 (2018) 185-194. https://doi.org/ 10.1016/j.jclepro.2018.03.276.

[7] T.T. Qian, H. Jiang, Migration of Phosphorus in Sewage Sludge during Different Thermal Treatment Processes, ACS Sustain Chem Eng 2 (2014) 1411-1419. https://doi.org/10.1021/sc400476j.

[8] Y. Zhu, G. Zeng, P. Zhang, C. Zhang, M. Ren, J. Zhang, M. Chen, Feasibility of bioleaching combined with Fenton-like reaction to remove heavy metals from sewage sludge, Bioresour Technol 142 (2013) 530-534. https://doi.org/10.1016/j.biortech.2013.05.070.

[9] O. Marchenko, V. Demchenko, G. Pshinko, Bioleaching of heavy metals from sewage sludge with recirculation of the liquid phase: A mass balance model, Chem. Eng. J. 350 (2018) 429-435. https://doi.org/10.1016/j.cej.2018.05.174.

[10] E. Wisniowska, M. Wlodarczyk-Makula, The effect of selected acidic or alkaline chemical agents amendment on leachability of selected heavy metals from sewage sludge, Sci Total Environ 633 (2018) 463-469. https://doi.org/10.1016/j.scitotenv.2018.03.163.

[11] S. Petzet, B. Peplinski, P. Cornel, On wet chemical phosphorus recovery from sewage sludge ash by acidic or alkaline leaching and an optimized combination of both, Water Res 46 (2012) 3769-3780. https://doi.org/10.1016/j.watres.2012.03.068.

[12] B. Ebbers, L.M. Ottosen, P.E. Jensen, Comparison of two different electrodialytic cells for separation of phosphorus and heavy metals from sewage sludge ash, Chemosphere 125 (2015) 122-129. https://doi.org/10.1016/j.chemosphere.2014.12.013.

[13] L.M. Ottosen, P.E. Jensen, G.M. Kirkelund, Electrodialytic Separation of Phosphorus and Heavy Metals from Two Types of Sewage Sludge Ash, Sep. Sci. Technol.49 (2014) 1910-1920. https://doi.org/ 10.1080/01496395.2014.904347.

[14] W. Deng, J. Ma, J. Xiao, L. Wang, Y. Su, Orthogonal experimental study on hydrothermal treatment of municipal sewage sludge for mechanical dewatering followed by thermal drying, J. Cleaner Prod. 209 (2019) 236-249. https://doi.org/10.1016/j.jclepro.2018.10.261.

[15] X. Zhuang, Y. Huang, H. Liu, H. Yuan, X. Yin, C. Wu, Relationship between physicochemical properties and dewaterability of hydrothermal sludge derived from different source, J. Environ. Sci. 69 (2018) 261-270. https://doi.org/10.1016/j.jes.2017.10.021.

[16] Y. Xu, F. Yang, L. Zhang, X. Wang, Y. Sun, Q. Liu, G. Qian, Migration and transformation of phosphorus in municipal sludge by the hydrothermal treatment and its directional adjustment, Waste Manag 81 (2018) 196-201. https://doi.org/10.1016/j.wasman.2018.10.011.

[17] L. Wang, A. Li, Y. Chang, Hydrothermal treatment coupled with mechanical expression at increased temperature for excess sludge dewatering: Heavy metals, volatile organic compounds and combustion characteristics of hydrochar, Chem. Eng. J. 297 (2016) 1-10. https://doi.org/10.1016/j.cej.2016.03.131.

[18] F. Yang, S. Zhang, K. Cheng, M. Antonietti, A hydrothermal process to turn waste biomass into artificial fulvic and humic acids for soil remediation, Sci. Total Environ. 686 (2019) 1140-1151. https://doi.org/10.1016/j.scitotenv.2019.06.045.

[19] F. Yang, S. Zhang, J. Song, Q. Du, G. Li,N. V. Tarakina, M. Antonietti, Tackling the World's Phosphate Problem: Synthetic Humic Acids solubilize otherwise insoluble Phosphates for Fertilization,Angew. Chem. Int. Ed. 58 (2019) 18813-18816. https://doi.org/ 10.1002/anie.201911060.

[20] F. Yang, Q. Jiang, M. Zhu, L. Zhao, Y. Zhang, Effects of biochars and MWNTs on biodegradation behavior of atrazine by Acinetobacter lwoffii DNS32, Sci. Total Environ. 577 (2017) 54-60. https://doi.org/ 10.1016/j.scitotenv.2016.10.053.

[21] W. Jiang, X. Xing, X. Zhang, M. Mi, Prediction of combustion activation energy of NaOH/KOH catalyzed straw pyrolytic carbon based on machine learning, Renewable Energy 130 (2019) 1216-1225. https://doi.org/10.1016/j.renene.2018.08.089.

[22] W.D. Chanaka Udayanga, A. Veksha, A. Giannis, T.T. Lim, Pyrolysis derived char from municipal and industrial sludge: Impact of organic decomposition and inorganic accumulation on the fuel characteristics of char, Waste Manag 83 (2019) 131-141. https://doi.org/10.1016/j.wasman.2018.11.008.

[23] B. Usharani, N. Vasudevan, Eco-friendly approach for leaching out heavy metals from sewage sludge, Chem. Ecol. 32 (2016) 507-519. https://doi.org/ 10.1080/02757540.2016.1171320.

[24] S. Jeon, D. J. Kim, Enhanced phosphorus bioavailability and heavy metal removal from sewage sludge ash through thermochemical treatment with chlorine donors, J. Ind. Eng. Chem. 58 (2018) 216-221. https://doi.org/ 10.1016/j.jiec.2017.09.028.

[25] H. Zhang, J. Kovar, Fractionation of soil phosphorus, Methods of phosphorus analysis for soils, sediments, residuals, and waters 2 (2009) 50-60.

[26] Y. Lin, Y. Liao, Z. Yu, S. Fang, X. Ma, A study on co-pyrolysis of bagasse and sewage sludge using TG-FTIR and Py-GC/MS, Energy Convers. Manage. 151 (2017) 190-198. https://doi.org/ 10.1016/j.enconman.2017.08.062.

[27] Z. Li, H. Deng, L. Yang, G. Zhang, Y. Li, Y. Ren, Influence of potassium hydroxide activation on characteristics and environmental risk of heavy metals in chars derived from municipal sewage sludge, Bioresour.Technol.256 (2018) 216-223. https://doi.org/10.1016/j.biortech.2018.02.013.

[28] X. Wang, C. Li, Z. Li, G. Yu, Y. Wang, Effect of pyrolysis temperature on characteristics, chemical speciation and risk evaluation of heavy metals in biochar derived from textile dyeing sludge, Ecotoxicol. Environ. Saf. 168 (2019) 45-52. https://doi.org/10.1016/j.ecoenv.2018.10.022.

[29] W.P. Chan, J.Y. Wang, Formation of synthetic sludge as a representative tool for thermochemical conversion modelling and performance analysis of sewage sludge–Based on a TG-FTIR study, J. Anal. Appl. Pyrolysis 133 (2018) 97-106.

[30] N. Belmokhtar, H. El Ayadi, M. Ammari, L. Ben Allal, Effect of structural and textural properties of a ceramic industrial sludge and kaolin on the hardened geopolymer properties, Appl. Clay Sci.162 (2018) 1-9. https://doi.org/10.1016/j.clay.2018.05.029.

[31] Q. Du, G. Li, S. Zhang, J. Song, Y. zhao, F. Yang, High-dispersion zero-valent iron particles stabilized by artificial humic acid for lead ion removal, J. Hazard. Mater. 383 (2019) 121170. https://doi.org/10.1016/j.jhazmat.2019.121170.

[32] P. Illmer, A. Barbato, F. Schinner, Solubilization of hardly-soluble $AlPO_4$ with P-solubilizing microorganisms, Soil Biol. Biochem. 27 (1995) 265-270. https://doi.org/10.1016/0038-0717(94)00205-F.

[33] J. Havlin, S.L. Tisdale, W.L. Nelson, J.D. Beaton, Soil Fertility and Fertilizers- an Introduction to Nutrient Management, (1999).

[34] R.M. Town, H.P. Leeuwen, Van, B. Jacques, Chemodynamics of soft nanoparticulate complexes: Cu(II) and Ni(II) complexes with fulvic acids and aquatic humic acids, Environ. Sci. Technol. 46 (2012) 10487-10498. https://doi.org/10.1021/es3018013.

[35] W.D. Chanaka Udayanga, A. Veksha, A. Giannis, G. Lisak, V.W.C. Chang, T.-T. Lim, Fate and distribution of heavy metals during thermal processing of sewage sludge, Fuel 226 (2018) 721-744. https://doi.org/10.1016/j.fuel.2018.04.045.

[36] Y.J. Liang, L.Y. Chai, X.B. Min, C.J. Tang, H.J. Zhang, Y. Ke, X.D. Xie, Hydrothermal sulfidation and floatation treatment of heavy-metal-containing sludge for recovery and stabilization, J. Hazard. Mater. 217-218 (2012) 307-314. https://doi.org/ 10.1016/j.jhazmat.2012.03.025.

[37] C. Vogel, C. Adam, Heavy metal removal from sewage sludge ash by thermochemical treatment with gaseous hydrochloric acid, Environ. Sci. Technol. 45 (2011) 7445-7450. https://doi.org/ 10.1021/es2007319.

[38] J. Lehmann, M.C. Rillig, J. Thies, C.A. Masiello, W.C. Hockaday, D. Crowley, Biochar effects on soil biota–a review, Soil Biol. Biochem. 43 (2011) 1812-1836. https://doi.org/ 10.1016/j.soilbio.2011.04.022.

[39] M. Gebhardt, J.S. Fehmi, C. Rasmussen, R.E. Gallery, Soil amendments alter plant biomass and soil microbial activity in a semi-desert grassland, Plant Soil 419 (2017) 53-70. https://doi.org/ 10.1007/s11104-017-3327-5.

[40] K. Kasak, J. Truu, I. Ostonen, J. Sarjas, K. Oopkaup, P. Paiste, M. Kõiv-Vainik, Ü. Mander, M. Truu, Biochar enhances plant growth and nutrient removal in horizontal subsurface flow constructed wetlands, Sci. Total Environ. 639 (2018) 67-74. https://doi.org/ 10.1016/j.scitotenv.2018.05.146.